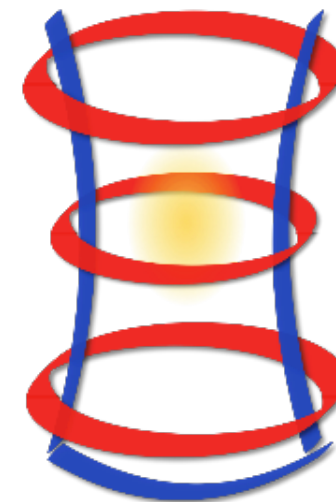
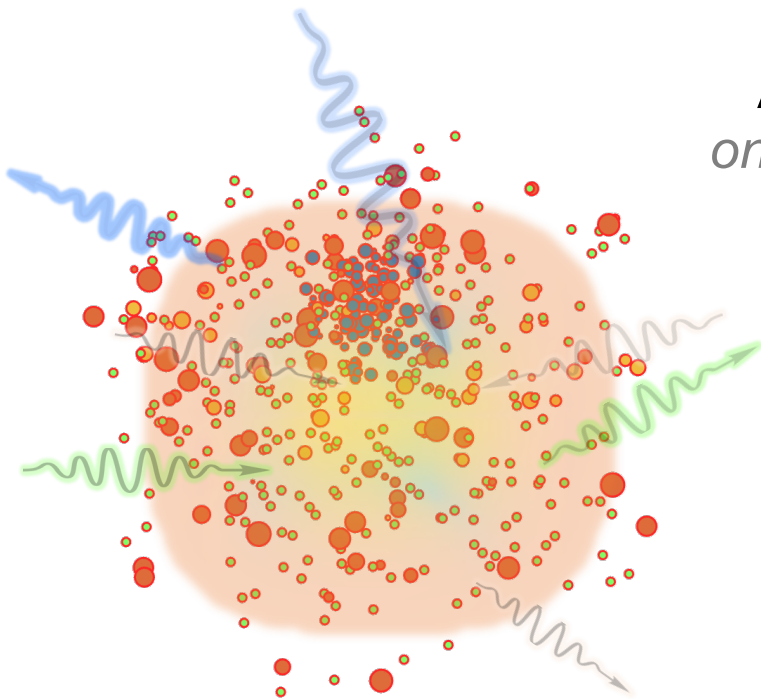


Numerical and experimental investigations on compact binary ejecta plasma opacity relevant for kilonova transient signals

Angelo Pivatella, INFN - LNGS

on behalf of the PANDORA collaboration



Plasmas for
Astrophysics
Nuclear
Decay
Observation and
Radiation for
Archaeometry

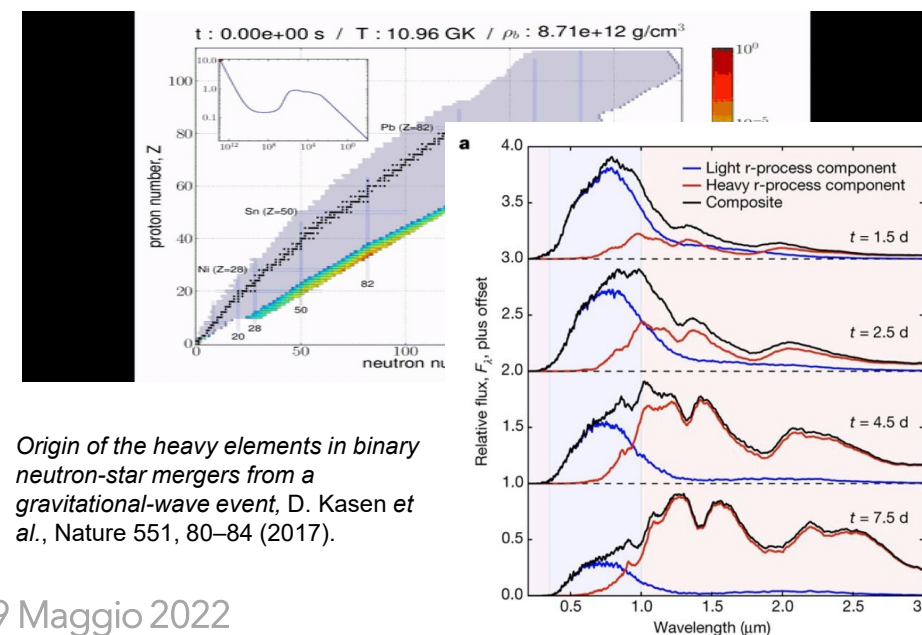


Motivation and introduction

- **Merger of binary neutron stars:** ejection of **n-rich matter**, rapid neutron capture (***r*-process**) nucleosynthesis
- **Radioactive decay** of synthesized *r*-process nuclei **power** electromagnetic transient: ***kilonovae* (KN)**
- Gravitational wave events (e.g., GW170817) from such merging detected along with KN counterpart AT2017gfo
- Detection of AT2017gfo spectrum: first direct evidence that these sites are among the major producer of nuclei heavier than iron via *r*-process
- **Plasma opacity** greatly **impacts** on energy **transport and spectroscopic observations** in many astrophysical environments
- Role played by the **opacity on KN emission**, as it delivers information on the post-merging plasma **ejecta composition** (*r*-process multi-components)
- **Large theoretical uncertainty** factor from an almost total ignorance on ejecta opacity at the typical conditions of a KN event



http://compact-merger.astro.su.se/Movies1/ns14_ns15_6mio_3D_density_v5.mov
<http://compact-merger.astro.su.se/Movies1/ns14ns15-6Mio-irrot-3Dcut-Ye-v2.mov>
<http://compact-merger.astro.su.se/Movies1/rProcessMoviexdiv4-12000.mov>



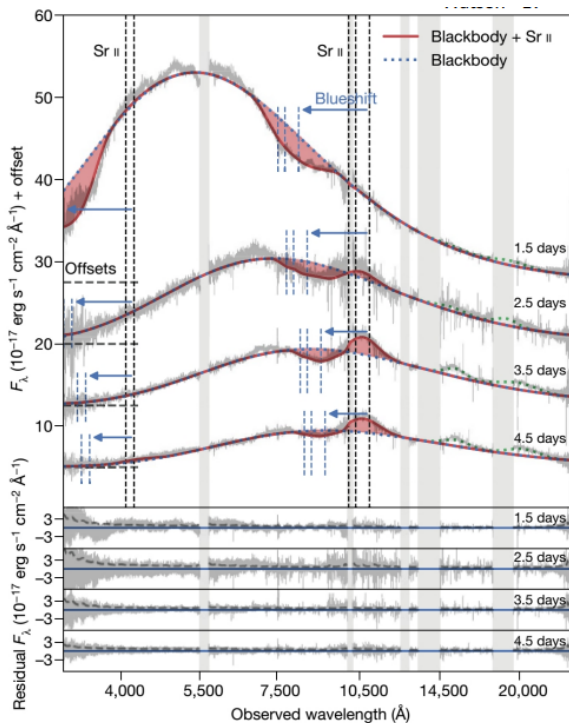
Origin of the heavy elements in binary neutron-star mergers from a gravitational-wave event, D. Kasen et al., Nature 551, 80–84 (2017).

GOAL

- Trapped magneto-plasmas conceived in **PANDORA** may open the route to **experimental in-laboratory measurements of opacities** at n_e and T_e resembling ejecta plasma conditions: **shed light on *r*-process** generated metallic species at **specific time-stages of KN diffusion**

State-of-the-art on r -process and KN

- Binary Neutron Stars (BNS) mergers are among major production sites of r -process elements
- Ejecta from BNS systems: first evidence of r -process nucleosynthesis in **kilonova (KN) AT2017gfo**, from Gravitational-Wave event **GW170817**
- **KN light-curve, 2 fundamental inputs: (1) r -process nucleosynthesis yields** (fixing the heating rate) **(2) opacity** (fixing the exchange of energy between plasma and radiation)



Watson, D., et al. Nature 574497-500, (2019)

$$\frac{dE}{dt} = -p \frac{dV}{dt} + \dot{\epsilon} - L(t)$$

(1) ←
← (2)

Opacity from **theoretical models**: **large uncertainty** factor, blending of many millions atomic transition lines, experimental data are largely desired!

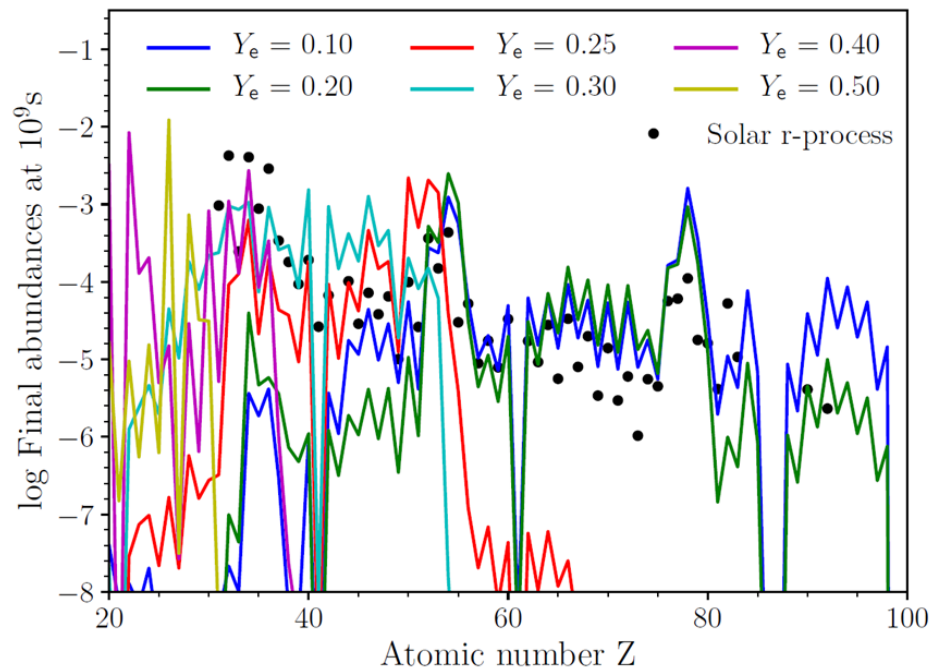
KN spectral analysis

- f-shell elements : strong blending of lines
 - Relativistic velocity : broad lines (multi-components and different velocities of ejecta)
 - Atomic data: incomplete and uncertain
- The analysis of the spectrum at **1.5 days** suggested the **presence of strontium** (Watson +19)

State-of-the-art on r -process and KN

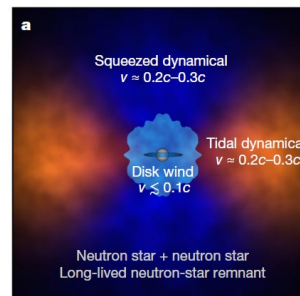
- r -process nucleosynthesis in BNS mergers

• Electron fraction, $Y_e \sim \frac{n_p}{n_p+n_n} \rightarrow$ **dominant parameter** (composition) \rightarrow **opacity**

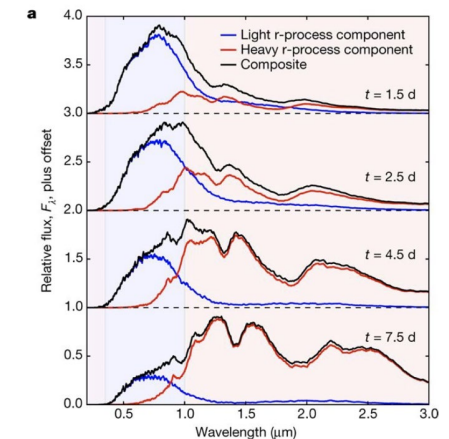


Pidatella, A., et al. Nuovo Cimento 44 C (2021) 65

- Production of lanthanides dramatically **changes photon opacity κ_ν**
- No lanthanides ($Y_e > 0.2$): low opacity, KN peak shaped mostly by light- r process elements, **blue-KN emission**
- Presence of lanthanides ($Y_e \leq 0.2$): larger opacity, KN peak shaped mostly by heavy- r process elements, **red-KN emission**

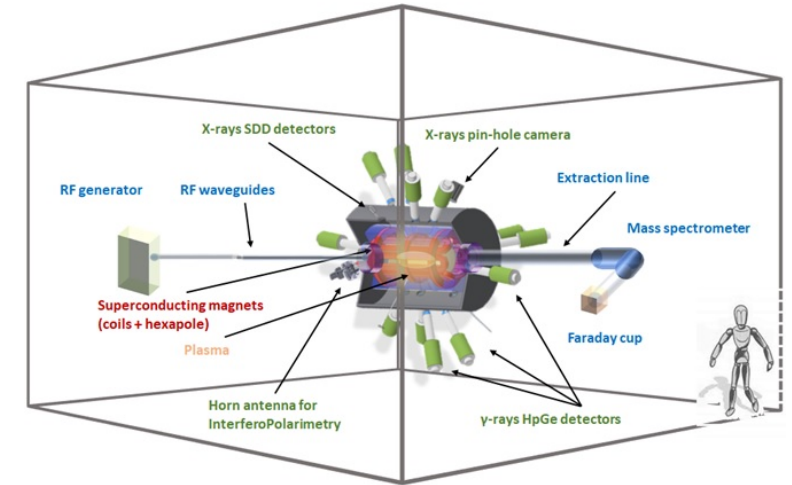


D. Kasen *et al.*, Nature 551, 80–84 (2017)



PANDORA: in-laboratory experimental measurements of NS² merger ejecta opacity

- **Trapped magneto-plasmas conceived in PANDORA:** experimental in-laboratory measurements of opacities at electron densities and temperatures resembling some **ejecta plasma conditions**
- **PANDORA concept:** compact **plasma trap** to magnetically confine ions of radioisotopes in a microwave-sustained plasma
- **Main Goal:** nuclear decay measurements in a plasma resembling **astrophysical conditions** (temperature, ion charge state distribution)
- **Multi-diagnostic setup:** **monitoring diagnostics + detectors array**



- **Electron dens:** $10^{10} - 10^{13} \text{ cm}^{-3}$
- **Electron Energy:** $\sim \text{eV} - 100 \text{ keV}$
- **Ion dens:** 10^{11} cm^{-3}

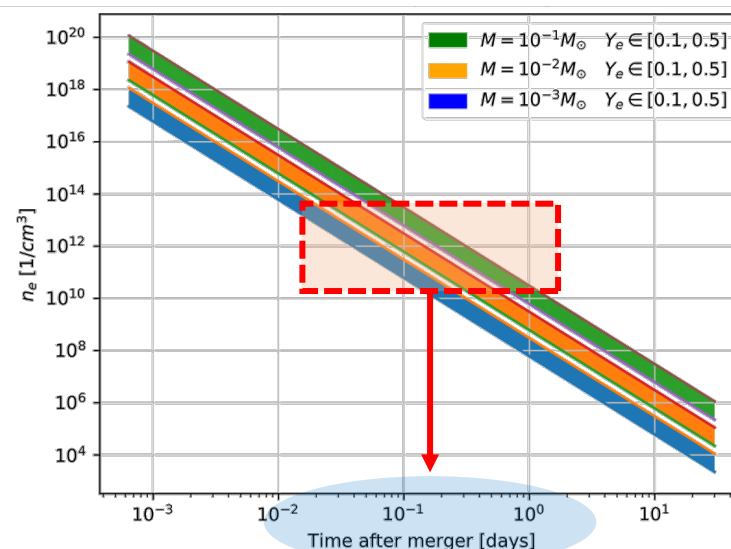
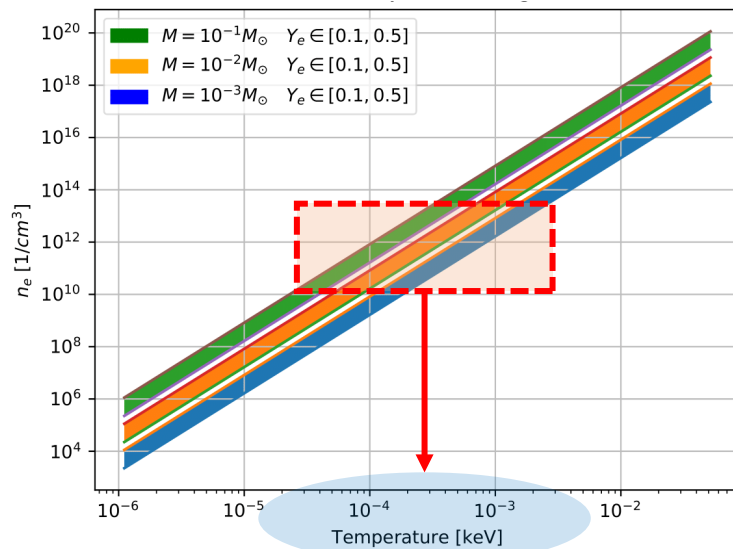
PHYSICS OF INTEREST FOR MMA
AND NUCLEAR ASTROPHYSICS

CAN BE DONE?

- s-process nucleosynthesis + β -decay branching
- r-process cosmic sites
- Nuclear reaction rates in stars
- Compact binary object spectroscopy (*kilonova transient*): to characterize composition and to identify GW events

PANDORA: in-laboratory experimental measurements of NS² merger ejecta opacity

- The KN emission is reprocessed by atomic opacities (mainly **bound-bound transitions**) to optical and infrared wavelengths. The emission in these wavelengths can probe the composition of the ejecta
- **Feasibility study**: astrophysical modelling BNS ejecta, nuclear network for nucleosynthesis yields, and population kinetics code for synthetic spectra



- **MODEL**: time-evolving ejecta through homologous expansion of a fluid element under adiabatic conditions (vs. mass M , temperature T , velocity v , and electron fraction Y_e)

- **Plasma density** in PANDORA: $10^{10-13} \text{ cm}^{-3}$
- **Plasma temperature** in PANDORA:
- few eV

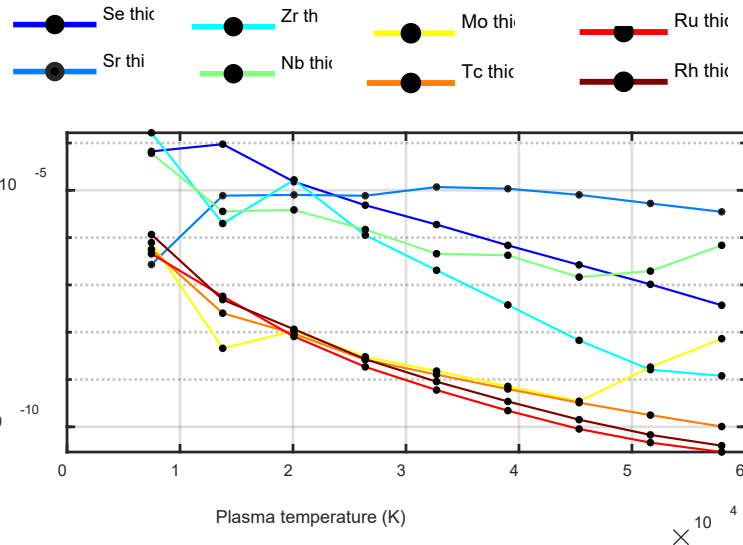
- **Time after merger**: from 10^{-2} up to 1 days
→ **blue-KN stage**

Pidatella, A., et al. Nuovo Cimento 44 C (2021) 65
 O. Korobkin *et al.*, Mon. Not. R. Astron. Soc., **426** (2012) 3-1940:1949
 D. Radice *et al.*, Astrophys. J., **869** (2018) 2-130
 J. Lippuner et al., Astrophys. J. Supplements, **233** (2017) 18

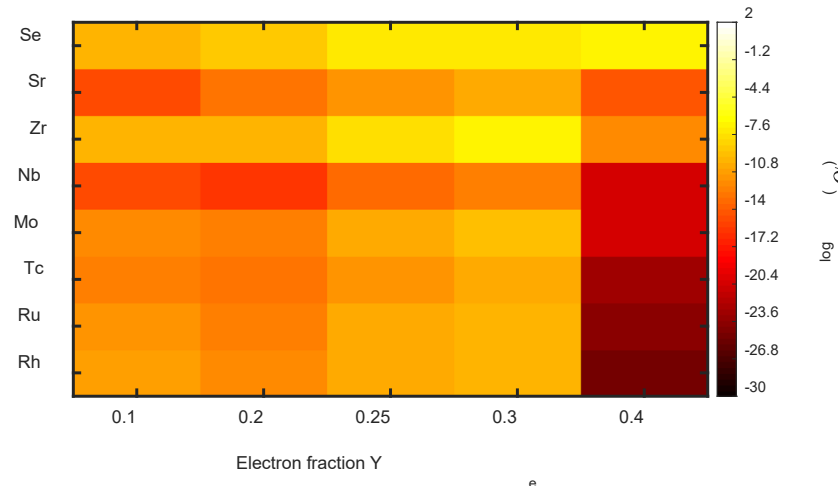
PANDORA: in-laboratory experimental measurements of NS² merger ejecta opacity

- The KN emission is reprocessed by atomic opacities (mainly **bound-bound transitions**) to optical and infrared wavelengths. The emission in these wavelengths can probe the composition of the ejecta
- Feasibility study:** astrophysical modelling BNS ejecta, nuclear network for nucleosynthesis yields, and population kinetics code for synthetic spectra

IDENTIFICATION OF PHYSICS CASES



Opacity weighted on abundances from SKYNET



- Time-dependent r-process elements abundances from SKYNET**, with distribution of ejecta properties (entropy, electron fraction and expansion timescale) from astrophysical simulations → **LIGHT R-PROCESS ELEMENTS, LOW NEUTRON RICHNESS**
- MEAN OPACITY vs. T**, weighted with abundances from SKYNET: **synthetic spectra of opacity from FLYCHK** → **Selenium, Strontium, Zirconium** most suitable for experiments

Pidatella, A., et al. Nuovo Cimento 44 C (2021) 65
 Chung H.-K. et al., High Energy Density Phys., 1 (2005) 3

PANDORA: in-laboratory experimental measurements of NS² merger ejecta opacity

- PANDORA is a **multi-diagnostic facility**: **optical emission spectroscopy (OES)** to probe plasma emission in the blue-KN stage, supported by ancillary non-invasive diagnostics
- Monitoring/measuring plasma parameters, plasma stability
- **Experimental setup and measurement design**

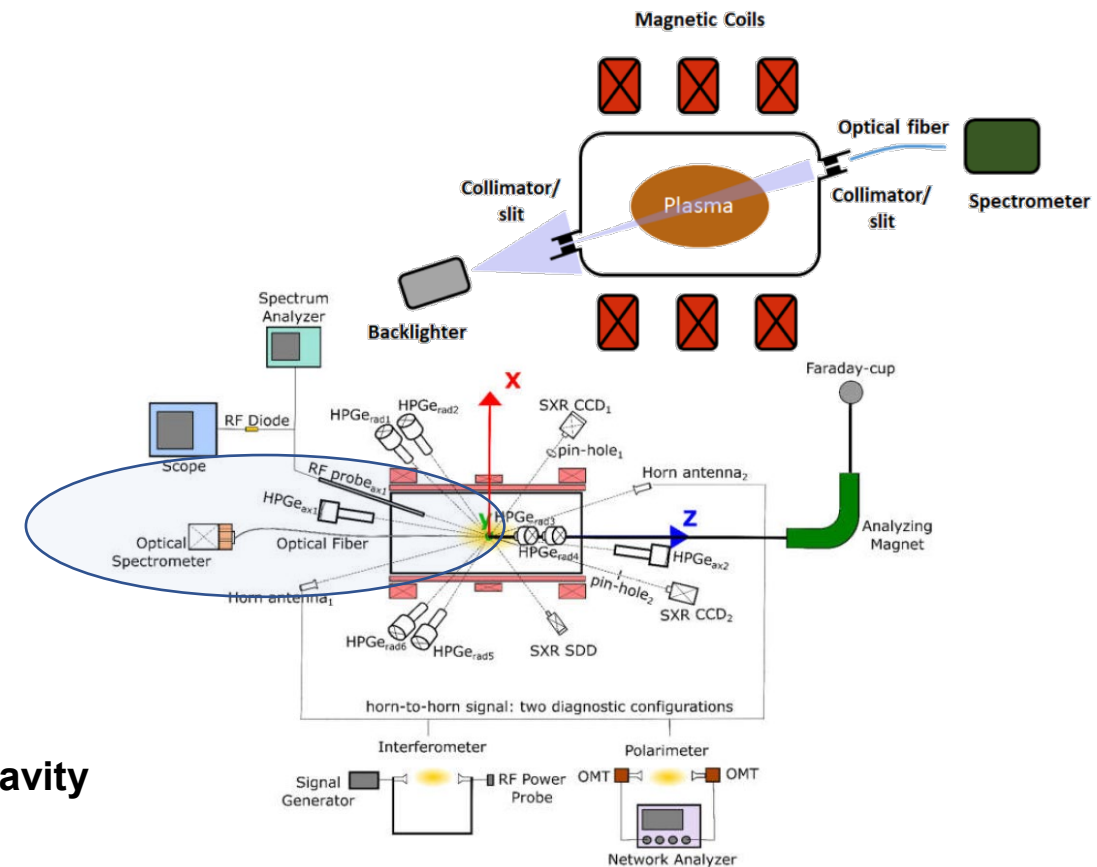
Opacity direct measurement: **TRANSMISSION**

$$T(\lambda) = \frac{I(\lambda)}{I_0(\lambda)} = e^{-\tau(\lambda)} = e^{-\int \kappa(\lambda, T_e(x), n_e(x)) \rho(x) dx}$$

\downarrow (green arrow) $\frac{I_{abs}(\lambda) - I_{se}^p(\lambda)}{I_0(\lambda)}$
 \downarrow (red arrow) $\kappa_s(\lambda, T, n) + \kappa_{abs}(\lambda, T, n)$

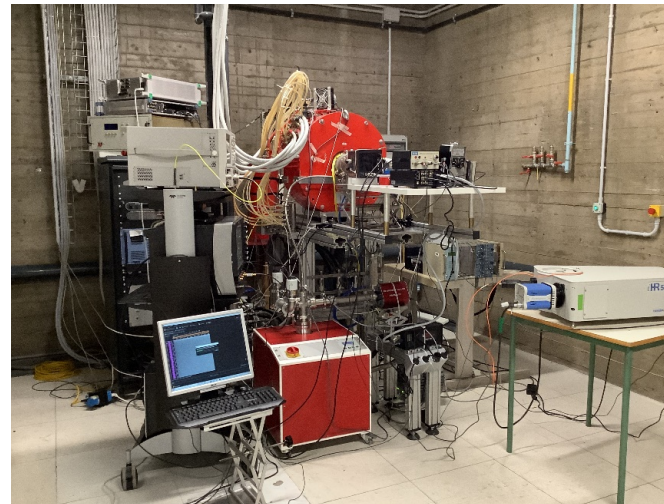
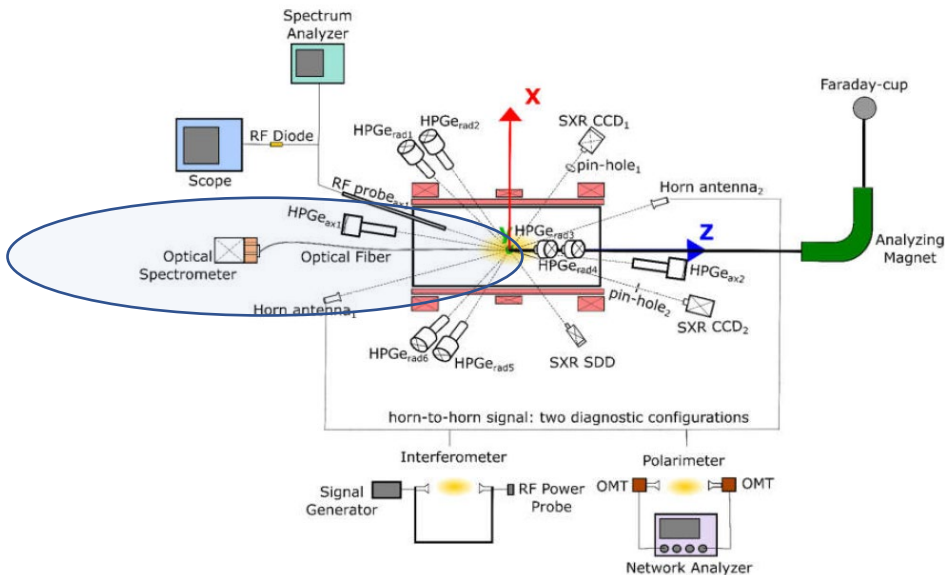
CHALLENGING

- **Transmission** measurements: plasma **active medium**
- **Self-emission** from plasma + radiation **attenuation** led by opacity
- **Spurious contribution**: (i) **reflection** at chamber wall, (ii) effect of **cavity** on wave propagation

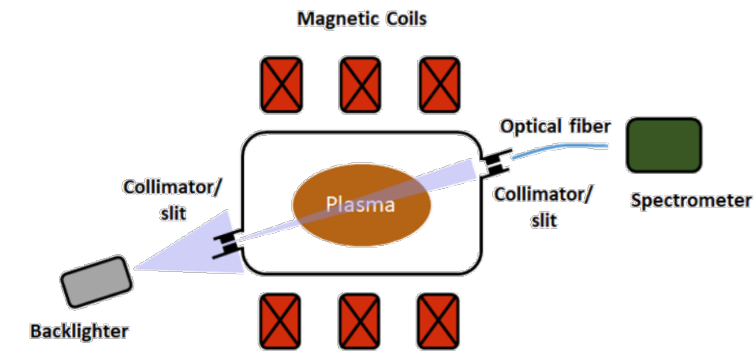


PANDORA: in-laboratory experimental measurements of NS² merger ejecta opacity

- PANDORA is a **multi-diagnostic facility**: **optical emission spectroscopy (OES)** to probe plasma emission in the blue-KN stage, supported by ancillary non-invasive diagnostics
- Monitoring/measuring plasma parameters, plasma stability
- **Experimental setup and measurement design**: w.i.p. on the **Flexible Plasma Trap**, first campaign of OES measurements



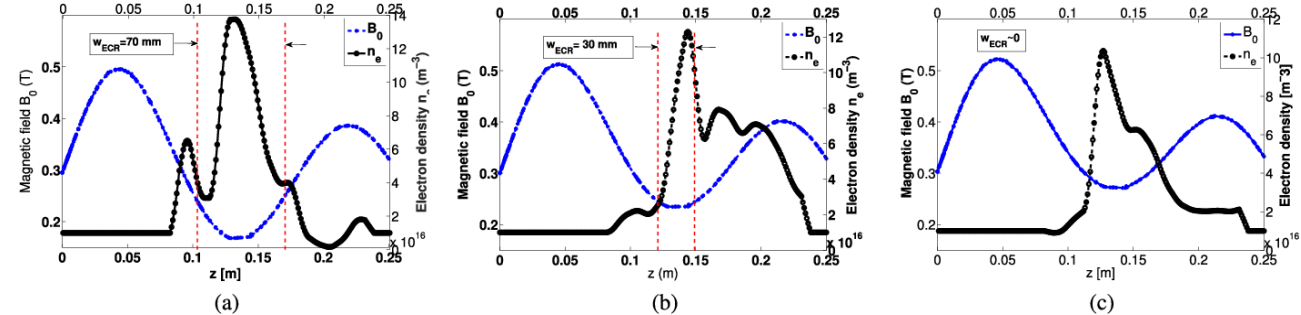
Flexible Plasma Trap @ LNS (setup Feb 2022)



FPT: diagnostic and theory for plasma characterization and opacity measurements

PLASMA TRAP CONFIGURATION (FPT vs. PANDORA):

- Simple mirror field, magnetic bottle (min-B field)
- RF power : 50÷450 W (up to 6 kW)
- Heating RF frequency: 3÷4 GHz (18÷21 GHz)



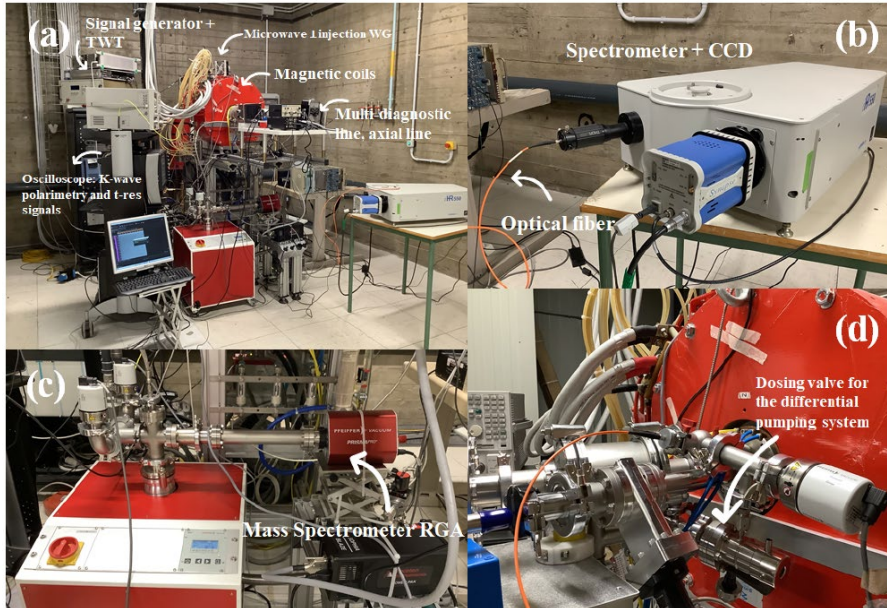
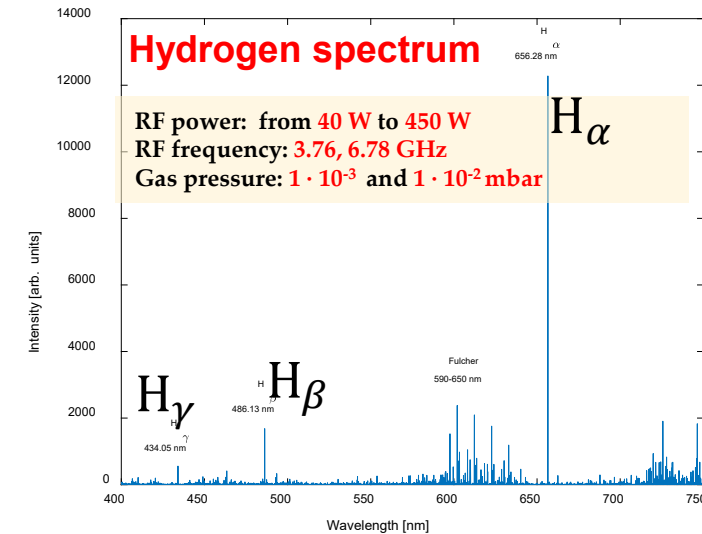
G. Torrisi et al., *IEEE Transactions on Antennas and Propagation*, vol. 67, no. 4, pp. 2142-2149, April 2019

- **Experimental H₂/Ar plasma characterization** performed on FPT: commissioning with **radial injection** and **high-power**

The comparison between the theoretical and experimental **line ratios** allows to evaluate the **plasma parameters (electron density and temperature)**

$$\boxed{H_\beta/H_\gamma, H_\alpha/H_\beta \quad n_e, T_e}$$

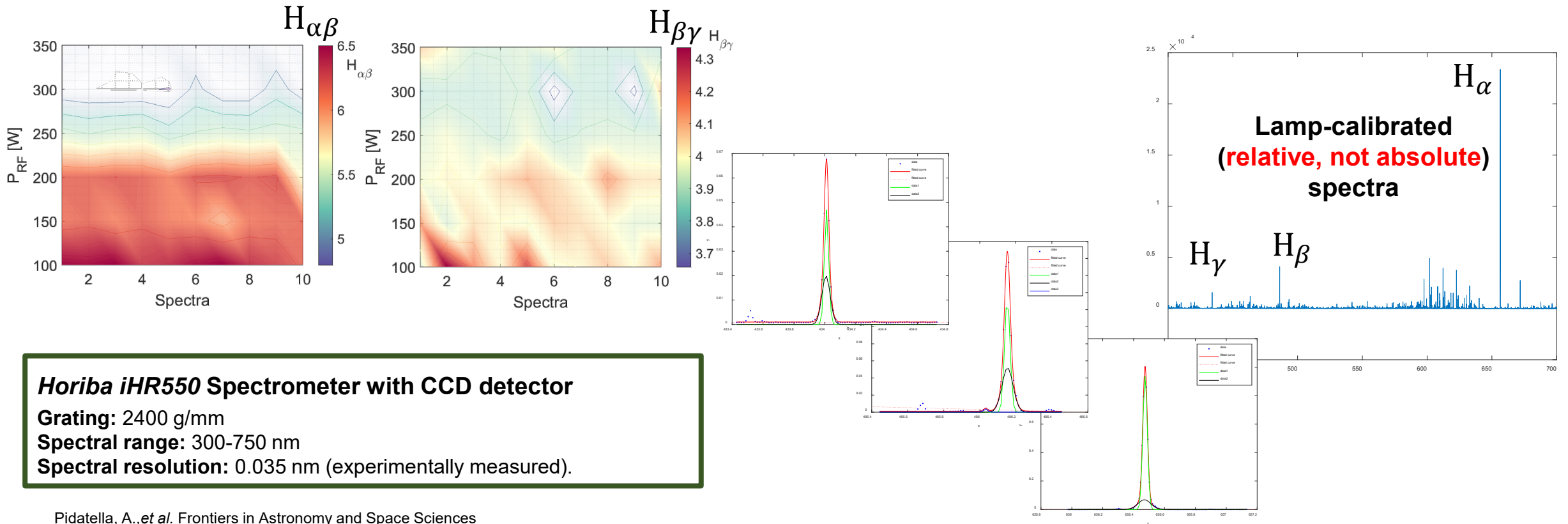
$$\frac{I_\alpha}{I_\beta} = \frac{\eta_\alpha \chi_\alpha(\rho, T)}{\eta_\beta \chi_\beta(\rho, T)} \rightarrow \langle \rho \rangle, \langle T \rangle$$



Pidatella, A., et al. *Frontiers in Astronomy and Space Sciences Nuclear Physics* (submitted)

FPT: diagnostic and theory for plasma characterization and opacity measurements

1. Monitoring plasma stability from emission line ratios

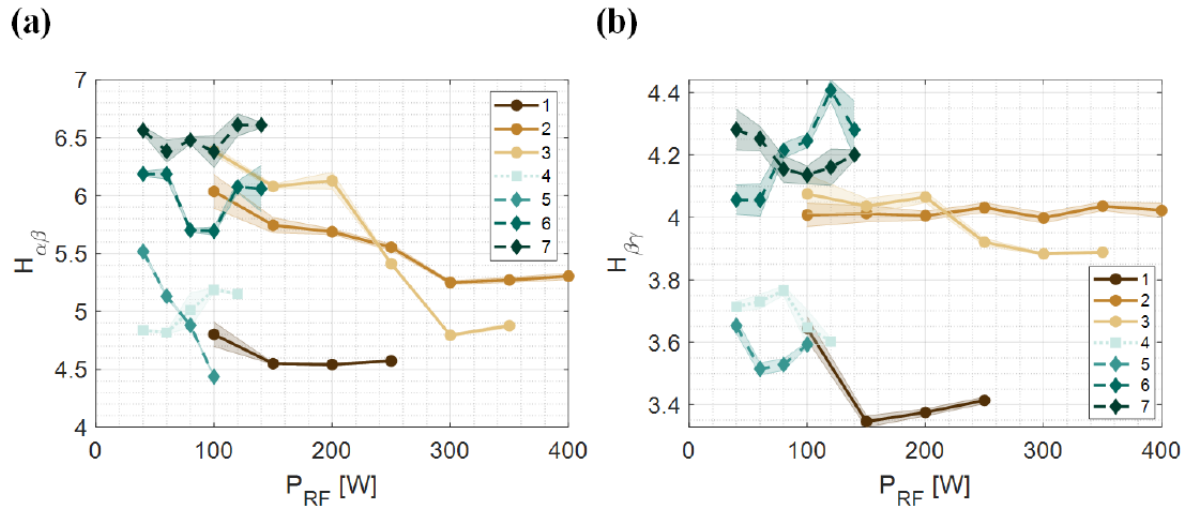


Horiba iHR550 Spectrometer with CCD detector
Grating: 2400 g/mm
Spectral range: 300-750 nm
Spectral resolution: 0.035 nm (experimentally measured).

Pidatella, A., *et al.* *Frontiers in Astronomy and Space Sciences*
Nuclear Physics (submitted)

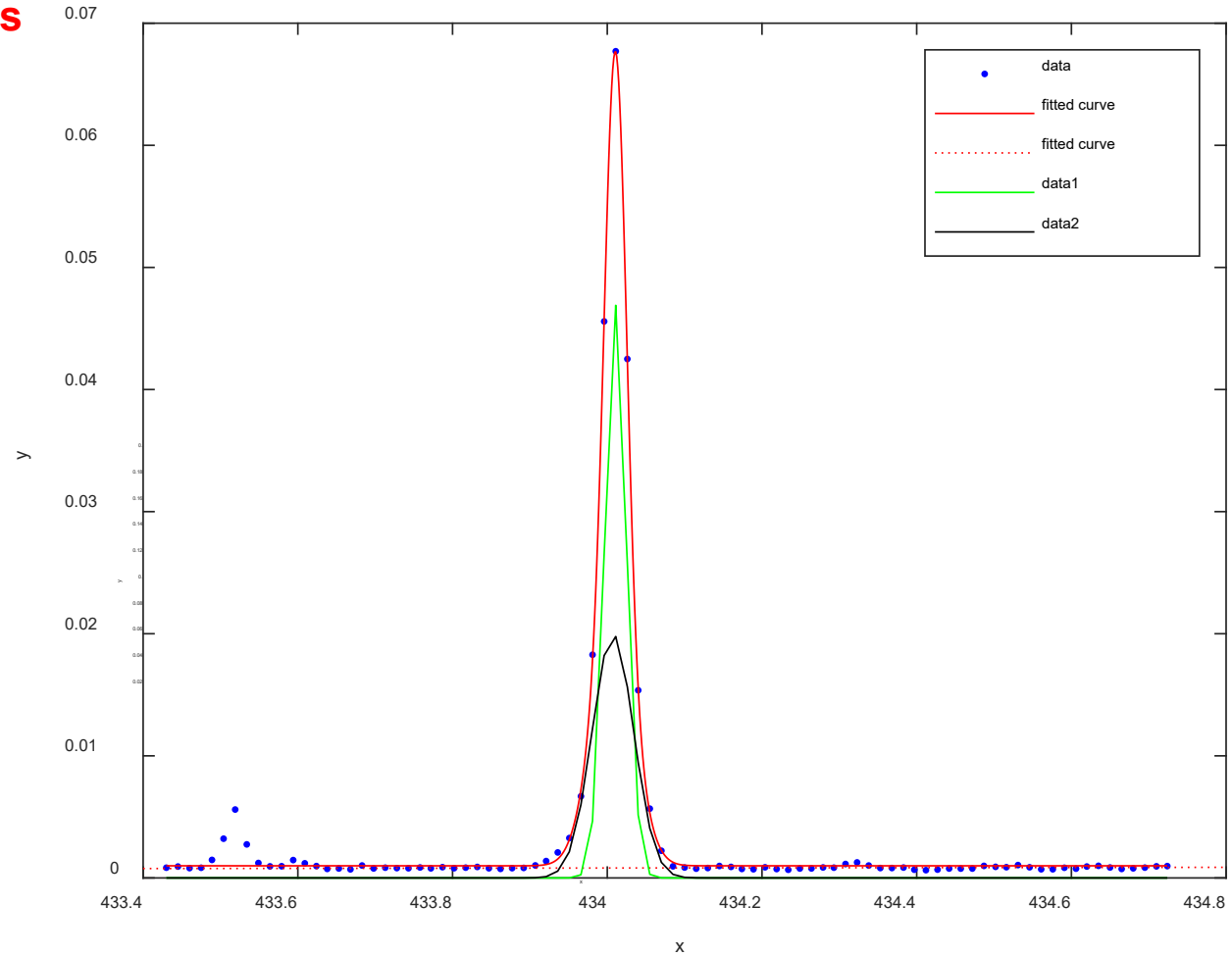
FPT: diagnostic and theory for plasma characterization and opacity measurements

1. Monitoring plasma stability from emission line ratios



Horiba iHR550 Spectrometer with CCD detector
Grating: 2400 g/mm
Spectral range: 300-750 nm
Spectral resolution: 0.035 nm (experimentally measured).

Pidatella, A., *et al.* *Frontiers in Astronomy and Space Sciences Nuclear Physics* (submitted)

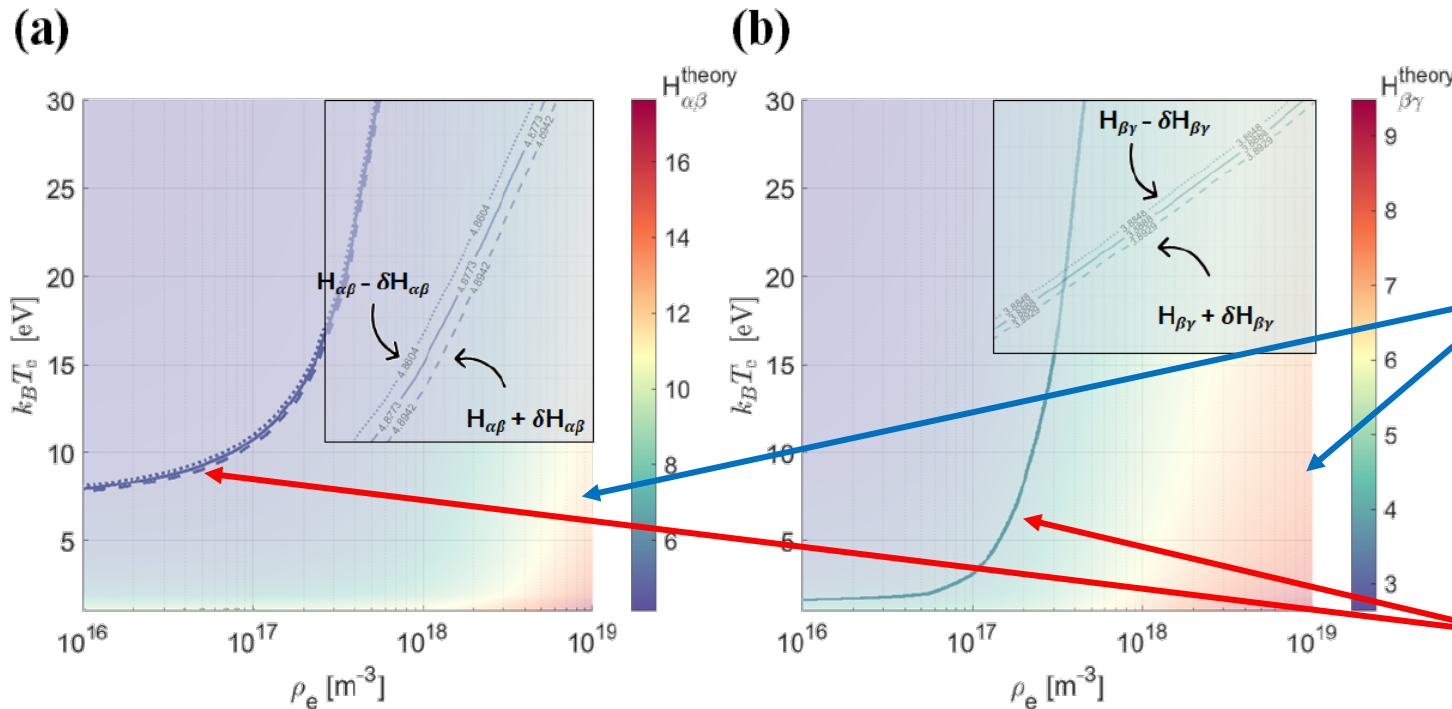


FPT: diagnostic and theory for plasma characterization and opacity measurements

1. Characterizing plasma density and temperature from line ratios

- **ESTIMATES** : Average density and temperature proportional to the **effective emission coefficients** χ_λ .

$$\frac{I_\alpha}{I_\beta} = \frac{\eta_\alpha \chi_\alpha(\rho, T)}{\eta_\beta \chi_\beta(\rho, T)} \rightarrow \langle \rho \rangle, \langle T \rangle$$



Thanks to the collaboration of colleagues from *MPI für Plasmaphysik* and *UNI-Augsburg*

Theory: YACORA CR model line ratios (n,T) isosurface

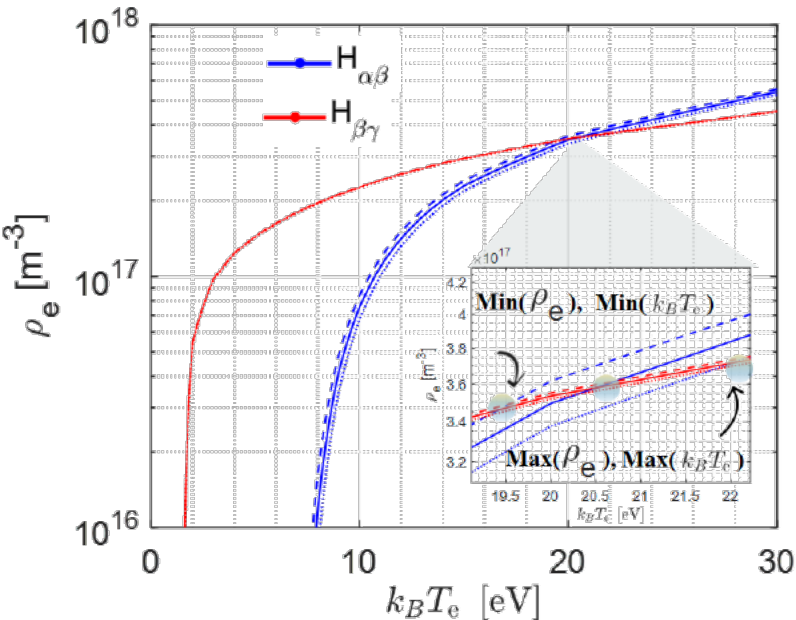
Collisional Radiative (CR) model
Balance eqs. are solved considering the different mechanisms of population and de-population of **atomic levels** (Rate eqs.)

Exp: measured line ratios, isoline on theoretical isosurface

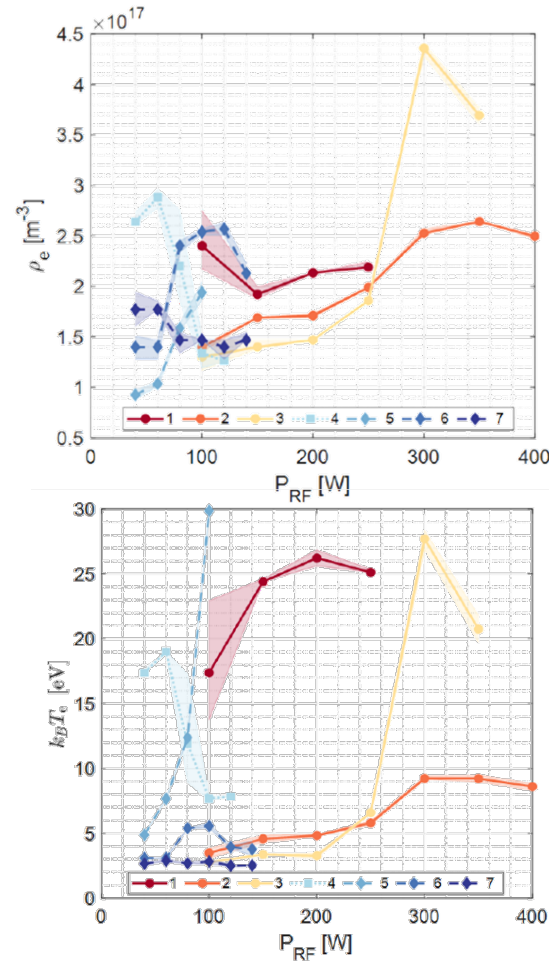
- Solving non-linear two-variables equation system from two-lines integrated ratios \rightarrow **cross point!**
Unique solution for $\langle \rho \rangle, \langle T \rangle$

FPT: diagnostic and theory for plasma characterization and opacity measurements

1. Characterizing plasma density and temperature from line ratios



Pidatella, A., et al. *Frontiers in Astronomy and Space Sciences Nuclear Physics* (submitted)



- **ESTIMATES** : Average density and temperature proportional to the **effective emission coefficients** χ_λ .

$$\frac{I_\alpha}{I_\beta} = \frac{\eta_\alpha \chi_\alpha(\rho, T)}{\eta_\beta \chi_\beta(\rho, T)} \rightarrow \langle \rho \rangle, \langle T \rangle$$

Thanks to the collaboration of colleagues from *MPI für Plasmaphysik* and *UNI-Augsburg*

Theory: YACORA CR model line ratios (n,T) isosurface

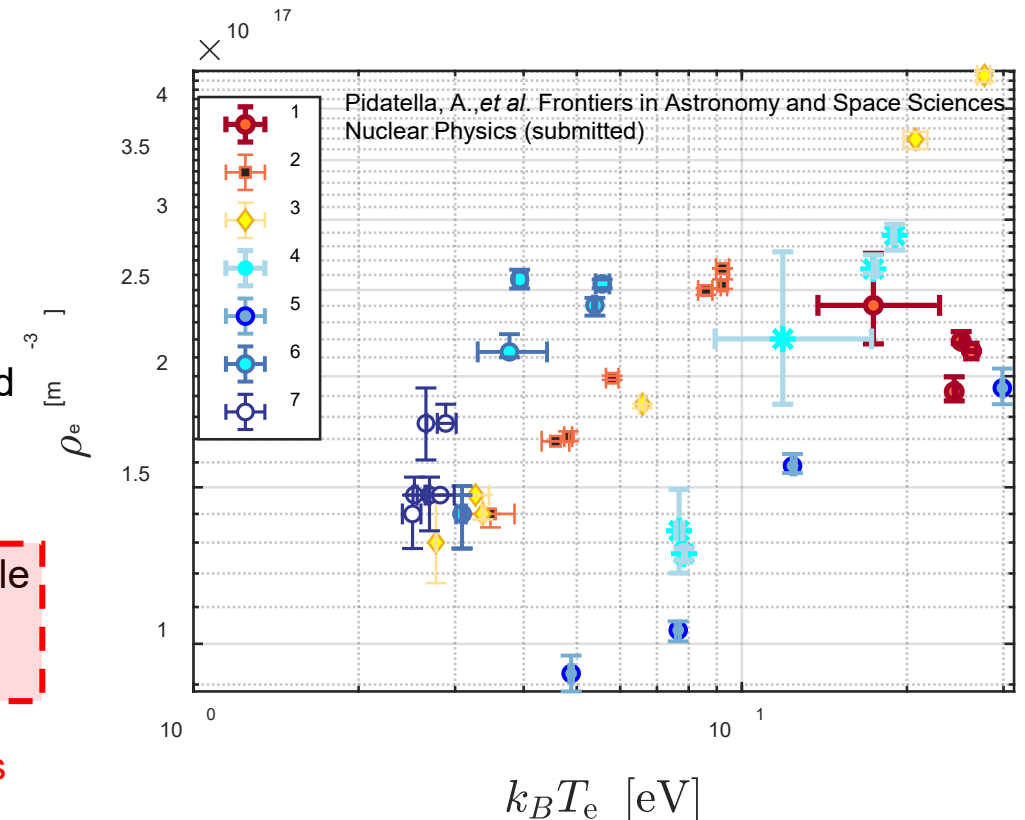
Collisional Radiative (CR) model
Balance eqs. are solved considering the different mechanisms of population and de-population of **atomic levels** (Rate eqs.)

Exp: measured line ratios, isoline on theoretical isosurface

- Solving non-linear two-variables equation system from two-lines integrated ratios \rightarrow **cross point!**
Unique solution for $\langle \rho \rangle, \langle T \rangle$

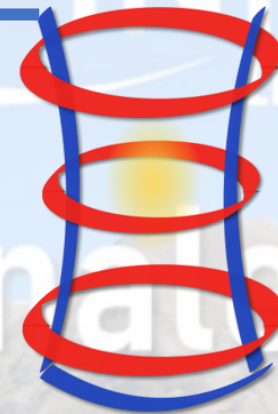
Summary and perspectives on KN opacity measurements

- Triggered by the astrophysical problem, a **feasibility study** to **measure for the first-time plasma opacity in ECR plasma** has been performed. **PANDORA** offers the conditions for reproducing **blue-KN peculiar environment**
- **PANDORA is a multi-diagnostic facility**: optical emission spectroscopy (OES) to probe plasma emission in the blue-KN stage, supported by ancillary non-invasive diagnostics
- Monitoring/measuring plasma parameters, plasma stability
- **Test-bench measurements** and experimental setups have been attempted on the **Flexible Plasma Trap @ LNS**
- **Plasma characterization** towards densities and temperatures suitable
- **Experimental difficulties**: active medium, resonant cavity, structured density and temperature profiles
- First data: using **line-ratio method**, **H-plasma + Ar-H mixtures**, estimate plasma parameters
- **Experimental setup and measurement design**: w.i.p. on the Flexible Plasma Trap, first campaign of OES measurements, closely reproducing KN conditions – **few eV, and 10^{11} cm^{-3}**
- **Perspectives**: **absolute calibration, light- r process elements plasmas (Se, Sr, Zr) opacity measurements via OES.**



Thank you for your attention!

Quinto Incontro Nazionale INFN Fisica Nucleare 2022



Plasmas for
Astrophysics
Nuclear
Decay
Observation and
Radiation for
Archaeometry



Also collaborating in the nuclear fusion research programme for the Divertor Tokamak Test (DTT) project

Backup I

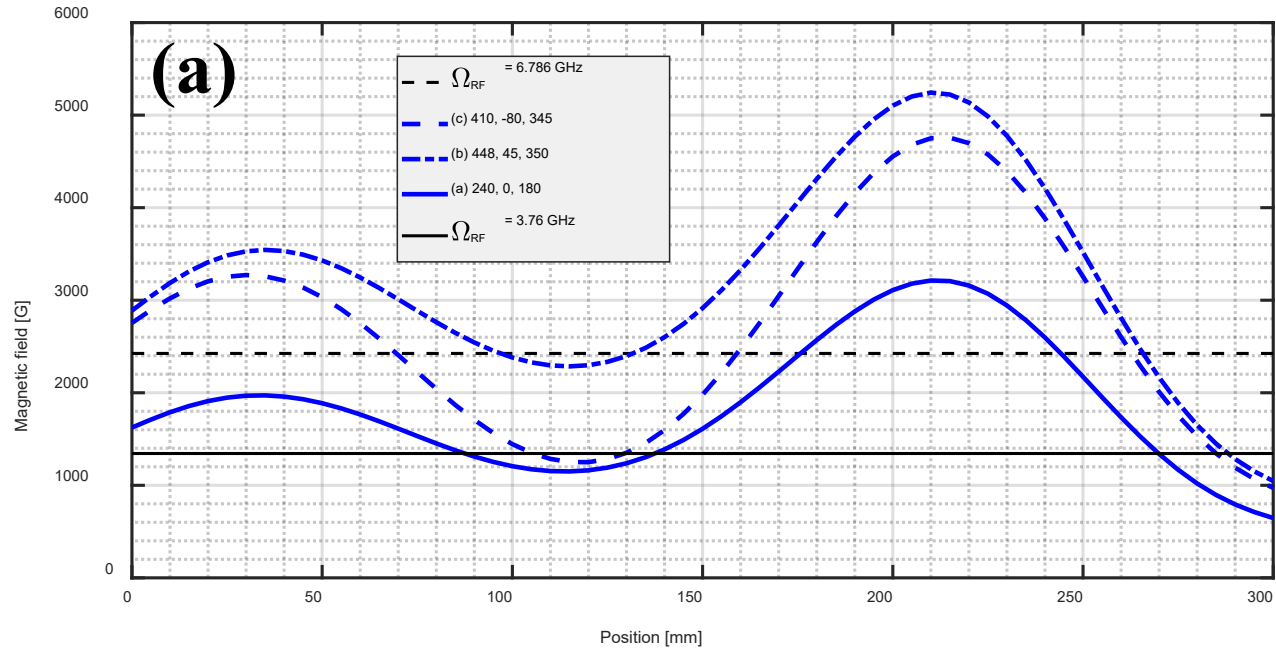
	B	f_{RF}	P_0							
P_{RF}	(a)	3.76	$9E-04$	100	150	200	250			
ρ_e	H₂			$2.40^{+2.17}_{-2.75}E17$	$1.92^{+2.00}_{-1.87}E17$	$2.13^{+2.13}_{-2.13}E17$	$2.19^{+2.24}_{-2.17}E17$			
$k_B T_e$				$17.38^{+13.76}_{-22.94}$	$24.40^{+24.60}_{-24.45}$	$26.22^{+25.61}_{-26.84}$	$25.12^{+25.26}_{-25.36}$			
P_{RF}	(a)	3.76	$1E-02$	100	150	200	250	300	350	400
ρ_e	H₂			$1.40^{+1.35}_{-1.40}E17$	$1.69^{+1.69}_{-1.69}E17$	$1.71^{+1.74}_{-1.69}E17$	$1.99^{+2.00}_{-1.98}E17$	$2.53^{+2.57}_{-2.51}E17$	$2.64^{+2.65}_{-2.64}E17$	$2.50^{+2.51}_{-2.47}E17$
$k_B T_e$				$3.48^{+3.08}_{-3.85}$	$4.56^{+4.31}_{-4.85}$	$4.83^{+4.75}_{-4.90}$	$5.80^{+5.65}_{-5.96}$	$9.23^{+9.15}_{-9.40}$	$9.22^{+8.98}_{-9.47}$	$8.60^{+8.32}_{-8.84}$
P_{RF}	(a)	3.76	$1E-02$	100	150	200	250	300	350	
ρ_e	H₂⁽⁹⁹⁾			$1.30^{+1.47}_{-1.17}E17$	$1.40^{+1.47}_{-1.38}E17$	$1.47^{+1.47}_{-1.47}E17$	$1.86^{+1.86}_{-1.84}E17$	$4.36^{+4.29}_{-4.41}E17$	$3.69^{+3.60}_{-3.77}E17$	
$k_B T_e$	+Ar⁽¹⁾			$2.77^{+2.76}_{-2.78}$	$3.37^{+3.35}_{-3.40}$	$3.27^{+3.09}_{-3.46}$	$6.50^{+6.49}_{-6.66}$	$27.70^{+26.88}_{-28.76}$	$20.74^{+19.72}_{-21.79}$	
P_{RF}	(b)	6.774	$1E-03$	40	60	80	100	120		
ρ_e	H₂			$2.64^{+2.74}_{-2.61}E17$	$2.88^{+2.96}_{-2.77}E17$	$2.20^{+1.86}_{-2.76}E17$	$1.34^{+1.49}_{-1.20}E17$	$1.26^{+1.28}_{-1.24}E17$		
$k_B T_e$				$17.37^{+17.63}_{-17.53}$	$19.00^{+19.02}_{-18.83}$	$11.88^{+8.94}_{-17.25}$	$7.69^{+7.81}_{-7.58}$	$7.85^{+7.83}_{-7.89}$		
P_{RF}	(c)	6.786	$1E-03$	40	60	80	100			
ρ_e	H₂			$0.93^{+0.97}_{-0.88}E17$	$1.03^{+1.06}_{-0.97}E17$	$1.58^{+1.63}_{-1.01}E17$	$1.94^{+2.04}_{-1.56}E17$			
$k_B T_e$				$4.88^{+4.84}_{-4.92}$	$7.66^{+7.58}_{-7.71}$	$12.37^{+12.33}_{-12.54}$	$29.86^{+29.99}_{-29.75}$			
P_{RF}	(c)	6.786	$1E-02$	40	60	80	100	120	140	
ρ_e	H₂			$1.40^{+1.50}_{-1.86}E17$	$1.40^{+1.47}_{-1.28}E17$	$2.40^{+2.45}_{-2.34}E17$	$2.54^{+2.57}_{-2.51}E17$	$2.57^{+2.63}_{-2.51}E17$	$2.13^{+2.23}_{-2.10}E17$	
$k_B T_e$				$3.09^{+3.09}_{-3.08}$	$3.09^{+3.01}_{-3.14}$	$5.40^{+5.35}_{-5.43}$	$5.56^{+5.41}_{-5.74}$	$3.93^{+3.84}_{-4.05}$	$3.77^{+3.30}_{-4.42}$	
P_{RF}	(c)	6.786	$1E-02$	40	60	80	100	120	140	
ρ_e	H₂⁽⁹⁹⁾			$1.77^{+1.94}_{-1.61}E17$	$1.77^{+1.86}_{-1.77}E17$	$1.47^{+1.54}_{-1.34}E17$	$1.47^{+1.47}_{-1.47}E17$	$1.40^{+1.47}_{-1.28}E17$	$1.47^{+1.54}_{-1.47}E17$	
$k_B T_e$	+Ar⁽¹⁾			$2.65^{+2.65}_{-2.66}$	$2.88^{+2.78}_{-3.01}$	$2.69^{+2.67}_{-2.70}$	$2.82^{+2.64}_{-2.99}$	$2.51^{+2.40}_{-2.60}$	$2.53^{+2.51}_{-2.56}$	

Pidatella, A., et al. *Frontiers in Astronomy and Space Sciences Nuclear Physics* (submitted)

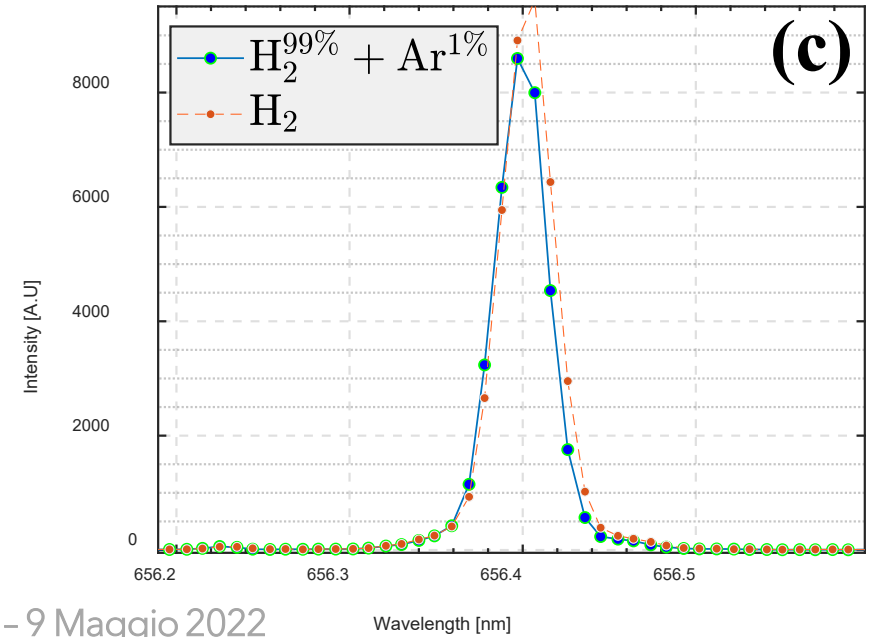
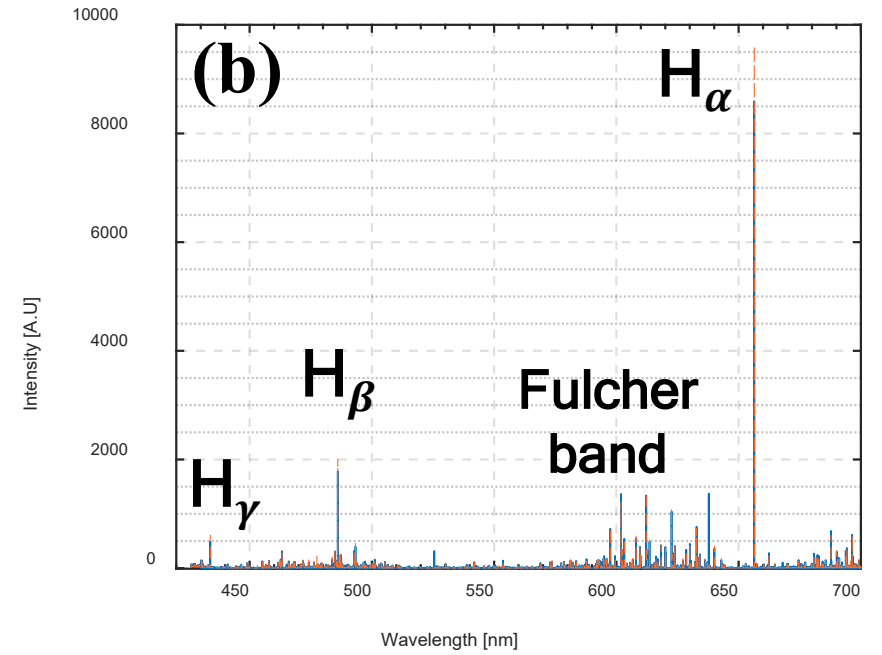
Table 2. OES experimental run details. Pure hydrogen (H₂) and Hydrogen-Argon mixture (H₂^{99%} + Ar^{1%}) cases are explicitly indicated. Configurations are labeled by n. (#) and B-field (a-c) - see also Fig. 2(a).

	$ B_{\text{max}}/B_{\text{min}} $	f_{RF} [GHz]	P_0 [mbar]	P_{RF} [W]	t_{acq} [s]	N. of spectra
# 1, (a), H ₂	2.7930	3.76	$9E-04$	$100 \div 250$	1	10
# 2, (a), H ₂	2.7930	3.76	$1E-02$	$100 \div 400$	1	10
# 3, (a), H ₂ ^{99%} + Ar ^{1%}	2.7930	3.76	$1E-02$	$100 \div 350$	1	10
# 4, (b), H ₂	2.2945	6.774	$1E-03$	$40 \div 120$	1	10
# 5, (c), H ₂	3.8289	6.786	$1E-03$	$40 \div 100$	2	5
# 6, (c), H ₂	3.8289	6.786	$1E-02$	$40 \div 140$	2	5
# 7, (c), H ₂ ^{99%} + Ar ^{1%}	3.8289	6.786	$1E-02$	$40 \div 140$	2	5

Backup 2



Pidatella, A., *et al.* *Frontiers in Astronomy and Space Sciences Nuclear Physics* (submitted)



Backup 3

Pidatella, A., *et al.* *Frontiers in Astronomy and Space Sciences*
 Nuclear Physics (submitted)

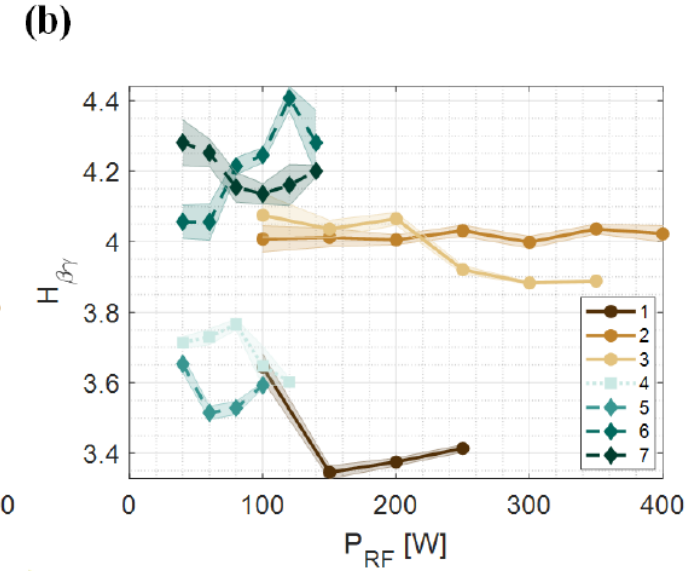
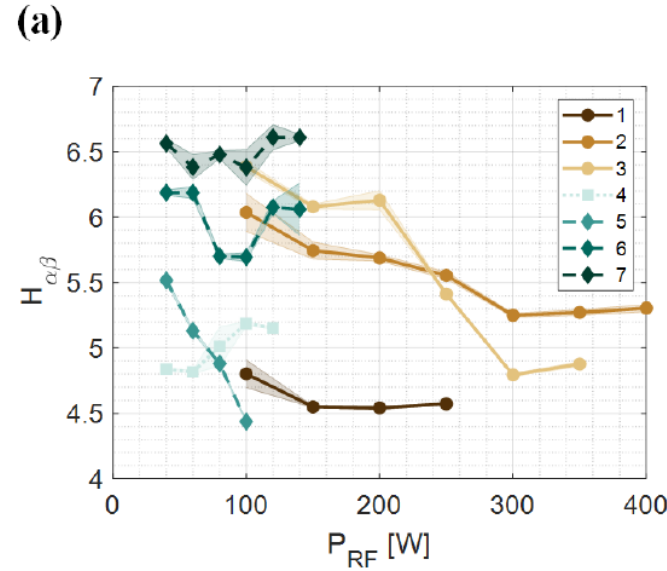
$$A_{\lambda_j} = \sum_{i=1}^N \frac{a_i \cdot c_i \cdot \sqrt{\pi}}{\Delta\lambda}$$

$$f(\lambda) = a \cdot \exp(-(\lambda - b)^2/c^2)$$

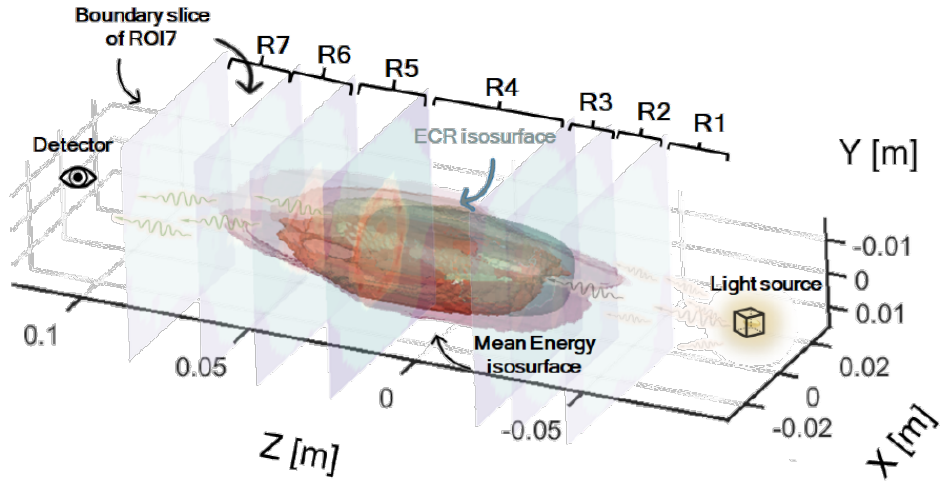
$$\delta A_{\lambda_j} = \sqrt{\sum_{i=1}^N \left[\left(\frac{\partial A_{\lambda_j}}{\partial a_i} \right)^2 \sigma_{a_i}^2 + \left(\frac{\partial A_{\lambda_j}}{\partial c_i} \right)^2 \sigma_{c_i}^2 \right]}$$

$$\delta H_{\alpha\beta} = H_{\alpha\beta} \sqrt{\left(\frac{\delta A_{\lambda_\alpha}}{A_{\lambda_\alpha}} \right)^2 + \left(\frac{\delta A_{\lambda_\beta}}{A_{\lambda_\beta}} \right)^2}, \quad \delta H_{\beta\gamma} = H_{\beta\gamma} \sqrt{\left(\frac{\delta A_{\lambda_\beta}}{A_{\lambda_\beta}} \right)^2 + \left(\frac{\delta A_{\lambda_\gamma}}{A_{\lambda_\gamma}} \right)^2}$$

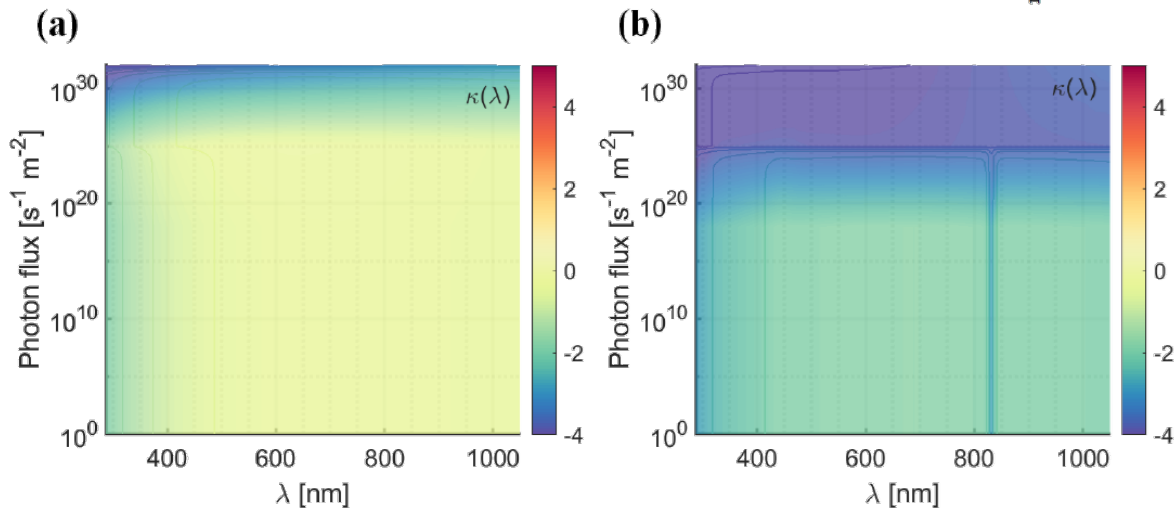
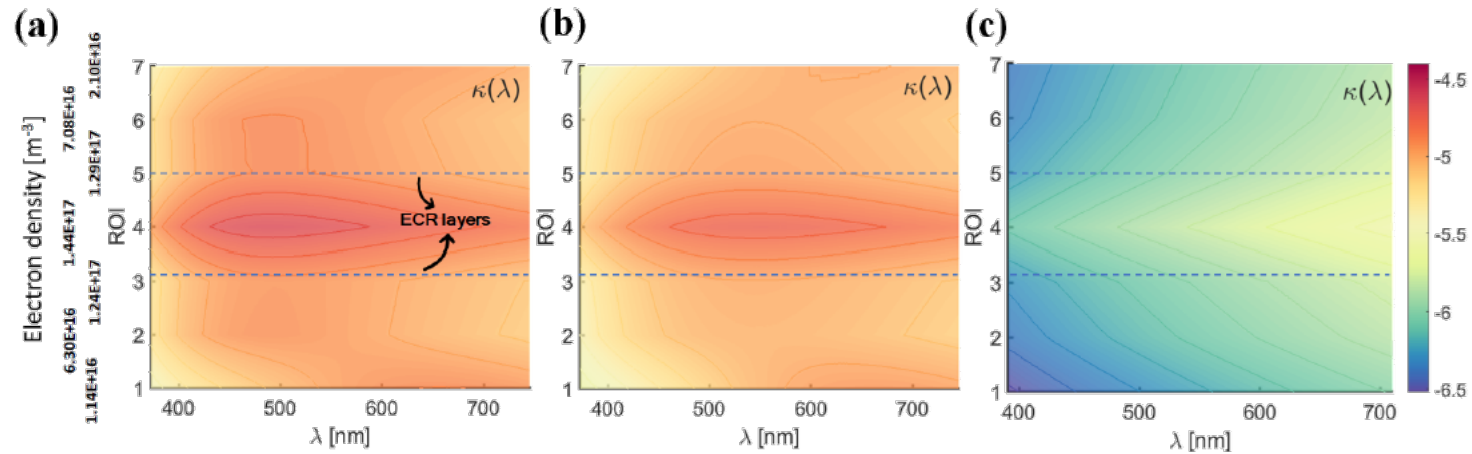
$$\langle H_{\alpha\beta, \beta\gamma} \rangle = \frac{\sum_{i=1}^S w_i^{\alpha\beta, \beta\gamma} H_{\alpha\beta, \beta\gamma}}{\sum_{i=1}^S w_i^{\alpha\beta, \beta\gamma}}, \quad \sigma_{\langle H_{\alpha\beta, \beta\gamma} \rangle}^2 = \frac{\sum_{i=1}^S w_i^{\alpha\beta, \beta\gamma} (H_{\alpha\beta, \beta\gamma} - \langle H_{\alpha\beta, \beta\gamma} \rangle)^2}{\sum_{i=1}^S w_i^{\alpha\beta, \beta\gamma}} \frac{n_{eff}}{n_{eff} - 1}, \quad \text{with } n_{eff} = \frac{\left(\sum_{i=1}^S w_i^{\alpha\beta, \beta\gamma} \right)^2}{\sum_{i=1}^S (w_i^{\alpha\beta, \beta\gamma})^2}$$



Backup 4



$$\kappa_{\lambda}^{BB} = N_e \left(1 - \frac{N_{u9l}}{N_{e9u}}\right) \frac{\pi e^2}{\rho m c} f_{lu} \varphi_{\lambda} \quad [\text{cm}^2 \text{g}^{-1}]$$



Pidatella, A., *et al.* *Frontiers in Astronomy and Space Sciences Nuclear Physics* (submitted)